MINERALOGICAL STUDY OF SOME ANTARCTIC MONOMICT EUCRITES, INCLUDING YAMATO-74356: A UNIQUE ROCK CONTAINING RECRYSTALLIZED CLASTIC MATRIX

Akira Yamaguchi[1,2] and Hiroshi Takeda[2]

[1]*Hawaii Institute of Geophysics and Planetology, School of Ocean and Earth Science and Technology, University of Hawaii at Manoa, Honolulu, HI 96822, U.S.A.*
[2]*Mineralogical Institute, Faculty of Science, University of Tokyo, Hongo, Bunkyo-ku, Tokyo 113*

Abstract: We studied the thermal and impact history of four Yamato Antarctic monomict eucrites, Yamato (Y)-74356, Y-791186, Y-792510, and Y-82037, by mineralogical techniques. Although the mineral chemistry of Y-74356 is typical of monomict eucrites, it contains a recrystallized clastic matrix similar to that of some lunar granulitic breccias. Y-74356 experienced shock brecciation during a major thermal event. In contrast, Y-791186 and Y-792510 have pyroxenes of the highest metamorphic degree but the clastic matrices are weakly recrystallized, *i.e.*, these two rocks were not extensively metamorphosed after breccia assembly. This indicates that the process that caused brecciation is distinct from the major thermal event. Y-82037 is a coarse-grained, unbrecciated ordinary eucrite, indicating that it was not affected by the brecciation event, except for the presence of a granoblastic portion in part of the pyroxene crystals.

We deduce that the thermal metamorphism that formed ordinary eucrites took place on a longer time scale and at a lower temperature than that which formed some lunar granulitic breccias. The precursors of these ordinary eucrites have suffered from smaller scale brecciation events than those of the lunar granulitic breccias (metamorphic polymict breccias). It is unlikely that there were comparably large cratering events on the small HED parent body to cause the strong thermal metamorphism. The thermal events may have taken place at a very early stage of the evolution of the primary crust of the HED parent body.

1. Introduction

Eucrites represent the meteoritic record of basaltic volcanism at a very early stage in the evolution of the solar system. The large asteroid 4 Vesta (520 km in diameter) has been considered as a possible parent body for the eucrites (*e.g.* Binzel and Xu, 1993). Many eucrites are monomict breccias composed predominantly of a single lithic type with homogenized pigeonites of uniform host composition and fine lamellae of exsolved augite. These are often called ordinary eucrites, by analogy with ordinary chondrites which are mostly equilibrated (Takeda *et al.*, 1978). Separate thermal metamorphism events are recorded in the clastic matrix and the pigeonite crystals in the clasts in some ordinary eucrites, indicating that the impact event responsible for the brecciation of the ordinary eucrites took place before or after the thermal event (Yamaguchi and Takeda, 1994; Metzler *et al.*, 1994).

167

Polymict eucrites are common in the early Antarctic meteorite collections (Takeda, 1991), but Yamato (Y)-74356 is the first monomict eucrite found in Antarctica and has been identified as a single equilibrated eucrite (Takeda, 1979). Subsequently, more monomict eucrites, such as Y-792510 and Y-791186, have been recovered from Antarctica (Takeda, 1991). Although Takeda (1979) and Takeda *et al.* (1981) showed that Y-74356 contains homogenized pyroxenes and a brief illustrated description was given by Yanai and Kojima (1987), this eucrite has not been studied in detail. During our comparative studies of lunar and eucritic granulitic breccias (Yamaguchi and Takeda, 1994), we found that Y-74356 has a completely recrystallized clastic matrix similar to those of some lunar granulitic breccias. To gain a better understanding of the early thermal event on the HED parent body, we investigated Y-74356 by mineralogical techniques and compared it to the other Antarctic monomict eucrites, Y-791186, Y-792510, and Y-82037.

2. Samples and Techniques

The sample of Y-74356 used in this study is the remainder of a potted butt of a chip (Y-74356,10) and a new PTS (Y-74356,62-2) provided by the National Institute of Polar Research (NIPR). Polished thin sections (PTSs) of Y-791186, Y-792510 and Y-82037 were supplied by NIPR and were examined by optical microscopy and a scanning electron microscope (SEM), JEOL JSM-840A equipped with an energy dispersive spectrometer (EDS) and a Kevex Super 8000 system. Chemical analyses were made by an electron probe microanalyser (EPMA) on a JEOL 8600 Super Probe at the Geological Institute of University of Tokyo and a JEOL JCXA-733 at the Ocean Research Institute, University of Tokyo. EPMA analyses were obtained at 15 kV and 12 nA with a focused beam using a correction program based on the procedure of Bence and Albee (1968). We observed the clastic matrix texture by back-scattered electron imaging (BEI) in the SEM.

3. Results

3.1. Y-74356

The Y-74356 eucrite (PTS,Y-74356,10 and 62-2) is a matrix-rich breccia (Fig. 1), composed of coarse-grained ($< 0.3 \times 0.7$ mm) clasts (CC) (Fig. 2), granulitic pyroxene (GP) clasts (Figs. 1 and 3), mineral fragments and granoblastic clastic matrix. The boundaries among lithic clasts are obscured by the effects of recrystallization. The CC-clasts are composed of pigeonite, lath-shaped plagioclase, and have tiny ($< 30 \ \mu$m in diameter) chromites. The granulitic clasts are composed of fine-grained ($< 80 \ \mu$m in diameter) polygonal pigeonite, augite, ilmenite and other minor minerals. Glasses other than fusion crust are not found in this PTS. Another section, Y-74356,62-1, has also been described to have a matrix-rich texture (Yanai and Kojima, 1987).

The photomicrograph of the clastic matrix in Y-74356 displays granoblastic texture (Fig. 1). The clastic matrix is dominated by two lithologies. One lithology is relatively dark in color and composed of pyroxene and plagioclase with modal abundance similar to the ordinary eucrites. The second lithology is light colored, rich
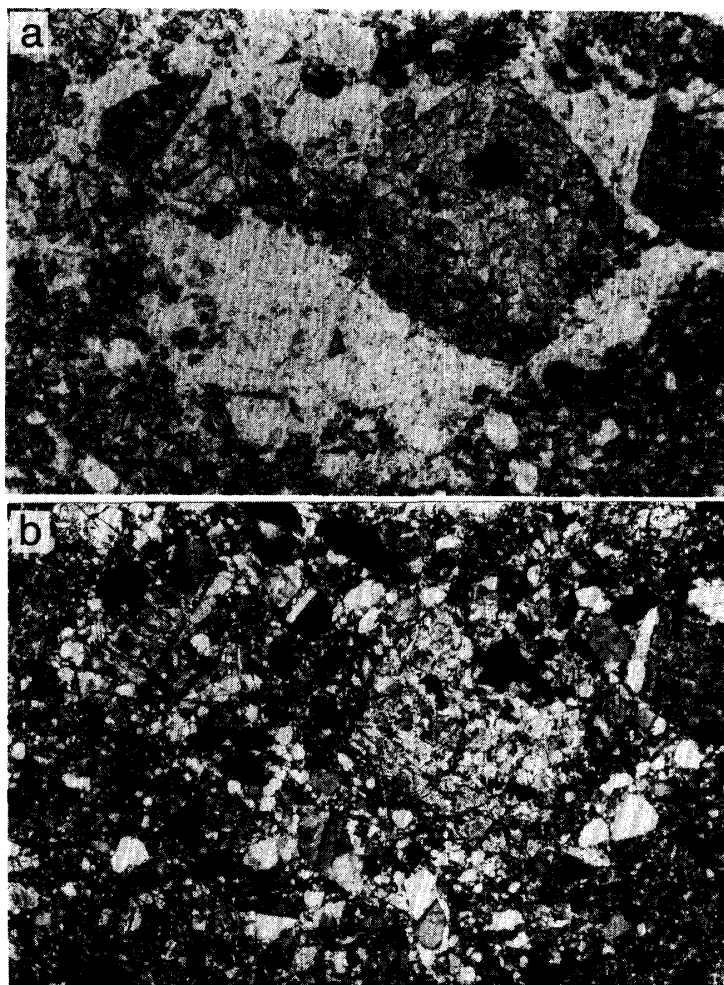
Fig. 1. Photomicrographs of granoblastic clastic matrix and granulitic pyroxene clast (middle, dark-colored) of Y-74356. (a) Plane light. (b) Same view under cross-polarizer, showing the granoblastic texture. Width of field is 3.0 mm.

Fig. 2. Photomicrograph of coarse-grained clast of Y-74356, showing cloudy pigeonite and plagioclase (white) under plane light. Width of field is 1.2 mm.
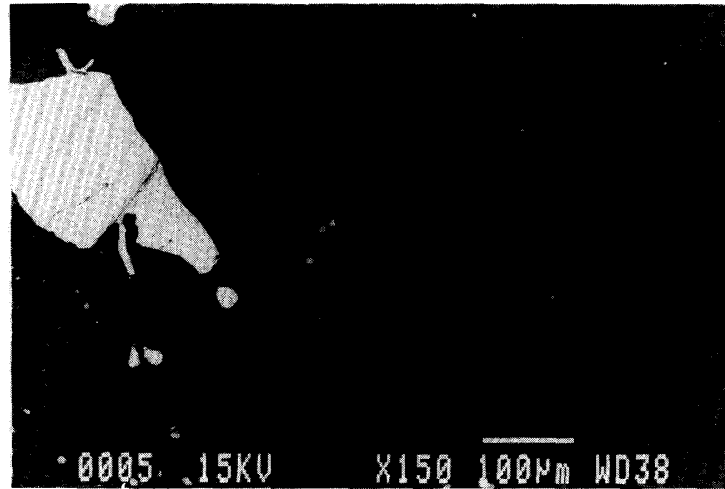
Fig. 3.   Backscattered electron image (BEI) of granulitic pyroxene clast of
          Y-74356, showing fine exsolution lamellae of augite in pigeonite and augite
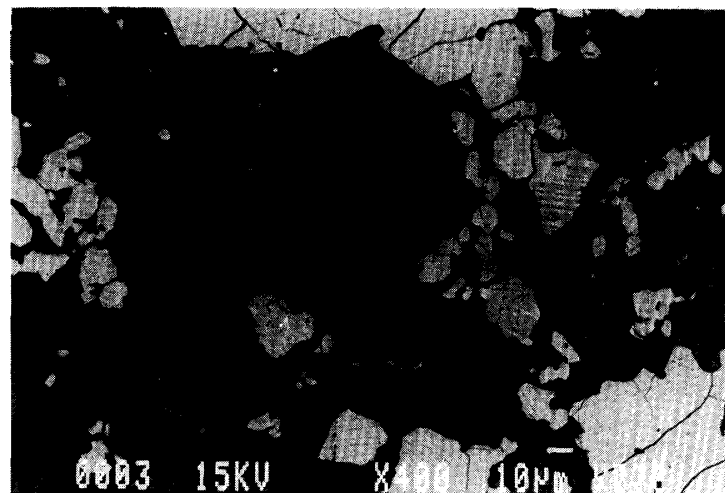   grains. Light gray: pigeonite; dark gray: augite; white: ilmenite.

Fig. 4.   BEI of granoblastic clastic matrix of Y-74356, shows smooth curved grain
          boundaries and porous nature of matrix. Dark gray: plagioclase; light
          gray: pyroxene; black: intergranular cavities.

in feldspathic mineral fragments and appears as a small region (< 3×2 mm). Small
crystals are anhedral and equant and their boundaries form smooth curves that
approach 120° triple junctures. Pore space (~10%) occurs sporadically in the form of
intergranular cavities (Fig. 4).

Many matrix pigeonites and pigeonites found in the CC-clasts have cloudy and
dusty cores, caused by fine crystals of chromite and ilmenite (MORI and TAKEDA,
1985), with transparent rims. These pigeonites also have closely-spaced augite (001)
lamellae. Tiny chromite crystals, less than 30 μm, are often found along a line in the
grain or subgrain boundaries of pigeonites. The GP-clasts have transparent pyroxenes
in which the pigeonites have very fine augite lamellae and some of the augites show
very fine exsolution texture (Fig. 3). Pyroxene compositions of whole PTS fall along a
single tie line in the pyroxene quadrilateral, ranging from $Ca_4Mg_{38}Fe_{58}$ to
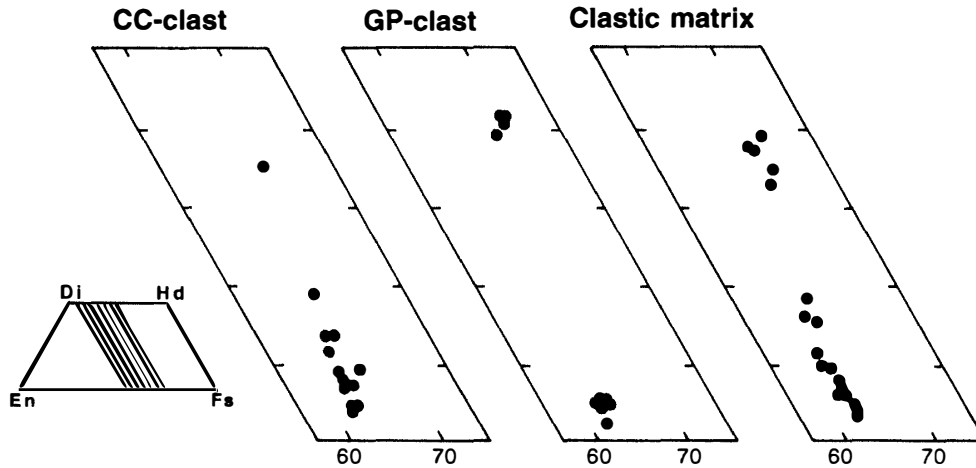
Fig. 5.   Pyroxene quadrilaterals of Y-74356 for coarse grained clast, granulitic pyroxene clast, and clastic matrix.

Table 1.   Chemical compositions (wt%) of pyroxene in Y-74356.

	CC-clast			GP-clast		Fragment		Clastic matrix	
	Host	Lam	Bulk*	Pig	Aug	1	2	1	2
SiO_2	50.0	51.0	49.2	50.1	51.7	49.7	49.4	50.0	51.1
Al_2O_3	0.36	0.46	0.39	0.24	0.73	0.33	0.26	0.31	0.42
TiO_2	0.24	0.36	0.30	0.28	0.44	0.17	0.26	0.16	0.14
FeO	33.8	18.9	32.5	33.7	16.8	33.5	29.7	33.7	30.2
MnO	1.14	0.60	1.07	1.04	0.55	1.08	0.92	1.02	0.94
MgO	12.3	10.4	11.7	12.3	10.3	12.2	12.0	12.5	11.9
CaO	1.67	17.1	3.43	1.82	19.7	1.94	5.28	1.67	5.75
Cr_2O_3	0.16	0.37	0.57	0.12	0.30	0.22	0.23	0.18	0.30
Total	99.7	99.2	99.1	99.6	100.5	99.1	98.1	99.5	100.8
Wo	3.7	36.9	7.6	4.0	41.8	4.3	11.7	3.7	12.5
En	37.9	31.2	36.1	37.8	30.4	37.7	37.0	38.3	36.1
Fs	58.4	31.8	56.3	58.1	27.8	58.0	51.3	58.0	51.4

*Determined by 30 μm broad beam.

$Ca_{37}Mg_{31}Fe_{32}$ (bulk composition: $Ca_8Mg_{36}Fe_{56}$) (Fig. 5 and Table 1). The variation of MnO versus FeO is shown in Fig. 6.

Many plagioclases have dusty inclusions at the subgrain boundary within the crystals. Extinction of the crystals is sharp or very weakly undulose. The chemical variation of matrix plagioclase fragments and plagioclase crystals in CC-clasts range from An_{86} to An_{94} (Fig. 7 and Table 2). Small, minor plagioclase grains in the GP-clast have high Na contents (An_{70}) (Table 2).

Minor minerals include ilmenite, chromite, silica minerals, and Fe-metal. Troilite is absent in this PTS. The chemical compositions of the tiny chromites at grain boundaries of the pyroxenes are $Fe_{6.8-7.9}Mg_{0.2}Mn_{0.1}Cr_{6.2-7.5}Al_{1.2-2.2}Ti_{1.0-2.1}O_{24}$. There are thin (< 10 μm in thickness) ilmenite ($Ti_{7.9}Fe_{7.3-7.5}Mn_{0.1-0.2}Mg_{0.4}O_{24}$)
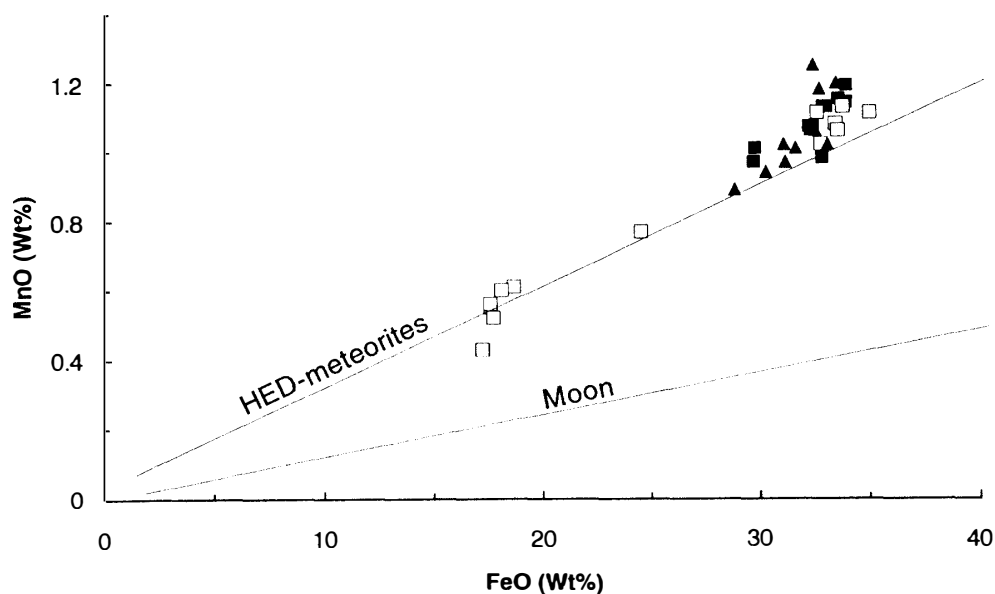
Fig. 6. MnO versus FeO plot (wt %) of the pyroxenes of Y-74356 for coarse-grained clast (solid squares), granulitic pyroxene clast (open squares), and clastic matrix (solid triangles).
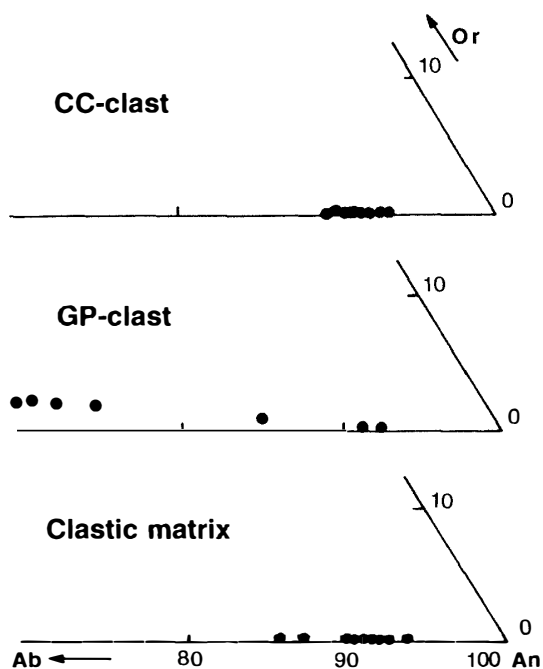

Fig. 7. Plagioclase compositions of Y-74356 for coarse-grained clast, minor plagioclase in granulitic pyroxene clast, and clastic matrix.

lamellae in large (100 μm in diameter) chromite crystal ($Fe_{8.4-8.9}Mg_{0.3}Mn_{0.1}Cr_{4.7-5.2}$ $Al_{1.0-1.2}Ti_{2.9-3.2}O_{24}$) in one of the GP-clasts (Table 3).

From our EPMA data, we have estimated the temperature using the Ca-pyroxene thermometer of Kretz (1982). The compositions of the small augite (<80 μm) in the GP-area give an estimated temperature of 848–873 °C (mean 857±16 °C)

Table 2. Chemical compositions (wt%) of plagioclase in Y-74356.

| | CC-clast | | GP-clast | | Clastic matrix | | |
	Core	Rim	1	2	1	2	3
SiO$_2$	45.0	46.8	45.4	52.3	46.5	45.4	48.4
Al$_2$O$_3$	35.0	33.6	34.8	30.3	33.8	34.9	32.6
TiO$_2$	0.00	0.00	0.12	0.00	0.00	0.00	0.00
FeO	0.28	0.33	0.53	0.38	0.17	0.20	0.57
MnO	0.04	0.02	0.00	0.03	0.02	0.00	0.04
MgO	0.03	0.03	0.02	0.05	0.03	0.04	0.05
CaO	18.8	17.6	18.9	14.0	17.5	18.7	16.8
Na$_2$O	0.77	1.54	0.83	3.36	1.53	0.90	2.15
K$_2$O	0.05	0.11	0.05	0.40	0.09	0.04	0.15
Total	100.0	100.0	100.7	100.9	99.6	100.2	100.8
Or	0.3	0.6	0.3	2.3	0.5	0.2	0.9
Ab	6.9	13.6	7.3	29.6	13.6	8.0	18.6
An	92.8	85.8	92.4	68.1	85.9	91.8	80.5

Table 3. Chemical compositions (wt%) of ilmenite (Ilm) and chromite (Chr) in Y-74356.

| | GP1 | GP2 | |
	Ilm	Ilm	Chr
SiO$_2$	0.00	0.04	0.05
Al$_2$O$_3$	0.02	0.04	4.31
TiO$_2$	52.9	52.4	18.2
FeO	44.3	43.8	47.4
MnO	0.72	0.90	0.66
MgO	1.48	1.30	1.01
CaO	0.00	0.01	0.03
Cr$_2$O$_3$	0.08	0.85	26.9
Total	99.5	99.3	98.6

whose variation is the result of the presence of fine pigeonite lamellae in the augite grain. The temperature for the CC-clast is 798 °C, which is calculated from data obtained by analytical transmission electron microscope (ATEM) for thin augite lamellae in a pyroxene in a CC-clast (TAKEDA *et al.*, 1981). The reported uncertainty of the KRETZ thermometer is ±60°C.

3.2. Y-792510, Y-791186, and Y-82037

PTS Y-792510,91-2 consists of brecciated plagioclase and pyroxene crystals up to 1 mm in length. Also present are a number of distinct polymineralic clastic fragments up to 3 mm across which show a slightly deformed basaltic texture (Fig. 8). These fragments are angular and generally less shocked than the surrounding material. Throughout the thin section, the pyroxene and plagioclase crystals show distorted twin lamellae, shear deformation, and clouding. The plagioclase also shows slight undulose extinction, and no maskelynite was observed. Many pyroxene crystals are cloudy and contain extensive fine exsolution lamellae. Chromite and ilmenite crystals are highly variable in size, ranging from 0.02 to 0.2 mm. Well defined granulitic regions have not been detected, but pyroxene crystals at some grain boundaries and matrices are fractured to small granular grains with slight evidence of recrystallization. An assemblage of the granular grains looks like the beginning of a granoblastic texture.

The mesostasis area found in another PTS of Y-792510 is surrounded by plagioclase laths (1.8×0.31 mm in size) and irregular pyroxene grains. The matrix portion is recrystallized and now consists of a few irregular ilmenite grains (0.15 mm in diameter) and fine-grained transparent minerals (silica, pyroxene and Ca-phosphate) spotted with opaque minerals (troilite and ilmenite).
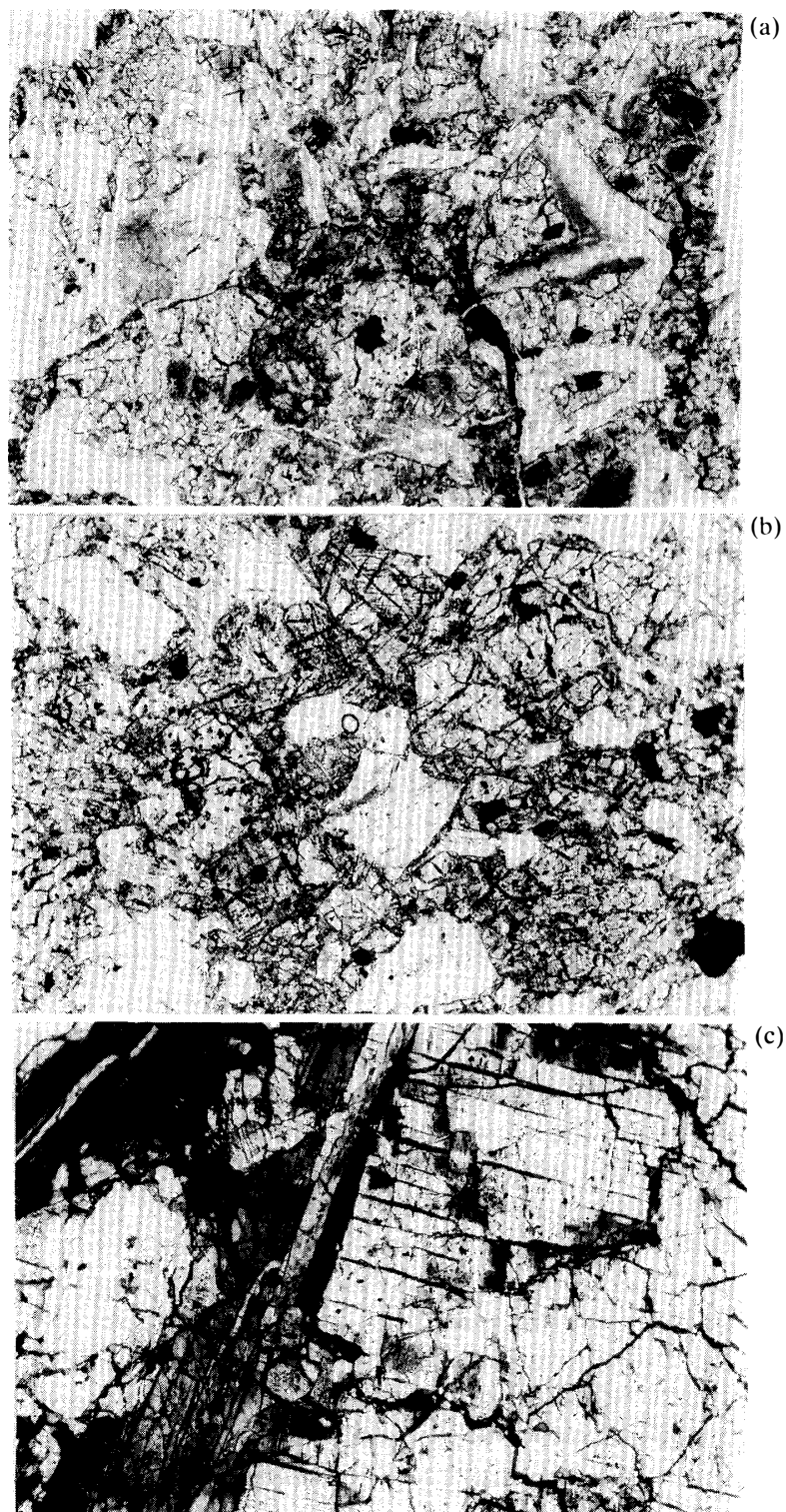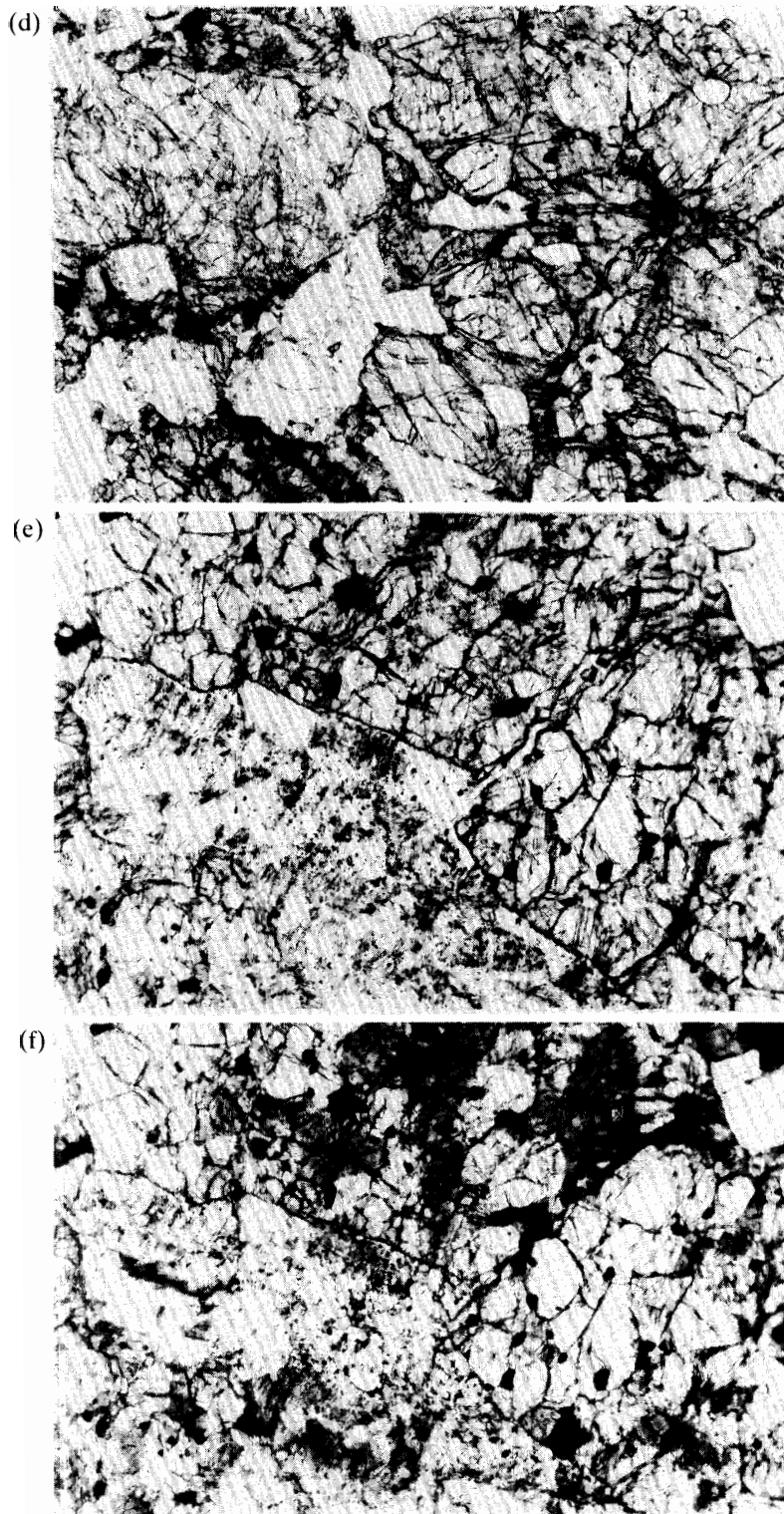
Fig. 8. Photomicrographs of Y-792510, Y-791186 and Y-82037.
(a) Overall view of Y-792510. Plane light. Width of field is 3.3 mm.
(b) Overall view of Y-791186. Plane light. Width of field is 3.3 mm.
(c) Partly inverted pigeonite crystal with exsolution lamellae. Cross polarized light. Width of field is 1.3 mm.

Fig. 8. (Continued).

(d) *Overall view of Y-82037. Width of field is 3.3 mm.*

(e) *Parts of pyroxenes with a granoblastic texture. Plane light. Width of field is 1.3 mm.*

(f) *Same view under cross polarizer, showing the granoblastic texture and exsolved pyroxene crystals without inclusions.*
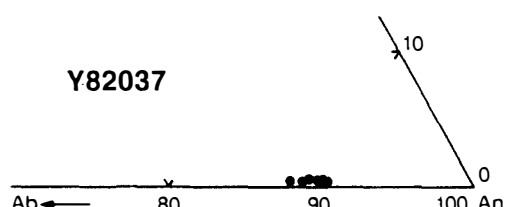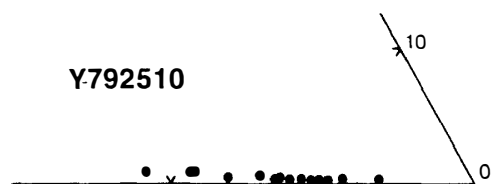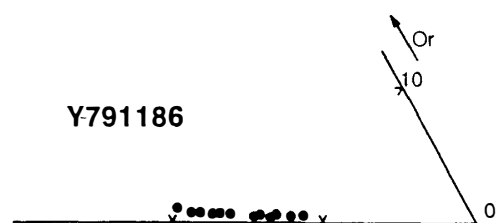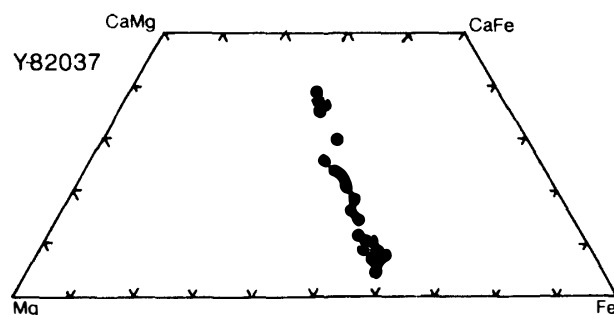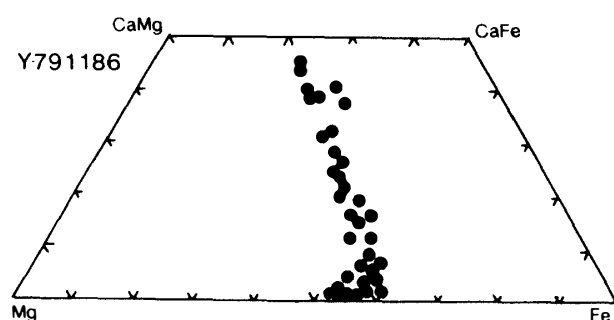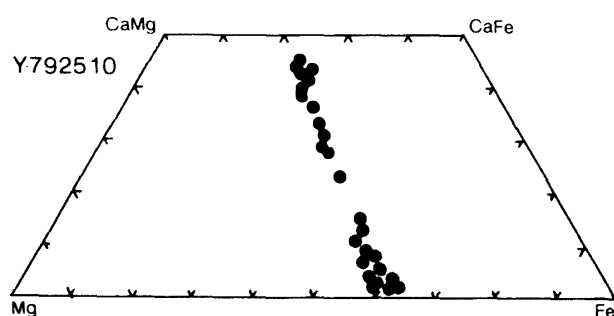
Fig. 9. Pyroxene quadrilaterals of Y-791186, Y-792510 and Y-82037.

Fig. 10. Plagioclase compositions of Y-791186, Y-792510 and Y-82037 plotted in parts of the Or-Ab-An diagrams.

Much of the low-Ca pyroxene in Y-792510 has the composition $Ca_2Mg_{35}Fe_{63}$, with a few analyses ranging up to $Ca_{15}Mg_{35}Fe_{50}$ (Fig. 9 and Table 4). Augites have compositions $Ca_{40-45}Mg_{30}Fe_{30-25}$. Some of the host pyroxenes are partly inverted to orthopyroxene. The plagioclase composition of Y-792510 ranges from An_{83} to An_{93}, and that of Y-791186 ranges from An_{80} to An_{92} (Fig. 10 and Table 5). These ranges are less than that of the type-1 eucrite Y-75011,84 (An_{78} to An_{90}) suggesting that they represent remnant zoning trends of the initial crystallization. Na-rich region is present in the core of a large crystal (Table 5).

PTS Y-791186,72-1 was previously described briefly by TAKEDA and GRAHAM (1991). This PTS shows a partially brecciated, coarse, subophitic texture and contains no mesostasis (Fig. 8). The pyroxenes often display well-developed "herring-bone"

Table 4.   Chemical compositions (wt%) of pyroxene in Y-791186, Y-792510 and Y-82037.

	Y-791186				Y-792510				Y-82037	
	Frag	Rep	Host	Lam	1	2	3	4	Gp	Bulk
SiO_2	51.4	51.5	50.9	52.6	50.3	49.2	50.2	51.9	49.1	49.5
Al_2O_3	0.35	0.40	0.17	0.39	0.28	0.31	0.13	0.04	0.48	0.49
TiO_2	0.13	0.30	0.13	0.22	0.10	0.56	0.09	0.23	0.44	0.47
FeO	28.2	22.1	33.7	14.6	32.5	32.4	35.9	15.97	32.6	31.1
MnO	0.94	0.44	1.11	0.45	1.05	1.05	1.11	0.53	1.16	1.11
MgO	13.2	11.3	12.9	10.9	11.5	11.2	11.8	10.2	12.1	12.0
CaO	5.51	13.3	1.19	21.5	4.21	4.65	0.74	21.3	3.55	4.62
Na_2O	0.02	0.05	0.00	0.06	0.02	0.02	0.00	0.05	0.00	0.02
K_2O	0.00	0.12	0.00	0.00	0.01	0.00	0.00	0.00	0.01	0.00
Cr_2O_3	0.12	0.10	0.13	0.21	0.11	0.27	0.11	0.24	0.25	0.22
Total	99.9	99.6	100.2	100.9	100.1	99.7	100.1	100.5	99.7	99.5
Wo	12.0	28.7	2.6	44.7	9.2	10.2	1.6	44.4	7.7	10.1
En	40.0	34.0	39.5	31.6	35.1	34.2	36.3	29.6	36.7	36.6
Fs	48.0	37.3	57.9	23.7	55.7	55.6	62.0	26.0	55.5	53.2

Rep: representative composition; Gp: granoblastic mean of pyroxene grains.

Table 5.   Chemical compositions (wt%) of plagioclase in Y-791186, Y-792510 and Y-82037.

	Y-791186			Y-792510			Y-82037
	Mean	Core Ca-rich	Core Na-rich	Dusty	Core Ca-rich	Core clear	Core
SiO_2	47.4	46.0	48.4	46.7	46.4	47.4	45.5
Al_2O_3	33.1	34.1	32.4	32.4	33.5	33.5	34.2
FeO	0.24	0.06	0.15	1.82	0.54	0.18	0.19
MnO	0.00	0.00	0.00	0.06	0.02	0.00	0.00
MgO	0.05	0.04	0.03	0.56	0.21	0.03	0.05
CaO	17.0	17.0	15.6	16.8	17.1	17.0	18.5
Na_2O	1.77	1.31	2.31	1.30	1.44	1.61	1.06
K_2O	0.16	0.07	0.33	0.10	1.07	0.11	0.07
Total	99.7	99.1	99.2	99.7	100.2	99.9	99.6
Or	0.9	0.4	1.9	0.7	0.4	0.6	0.4
Ab	15.7	11.9	20.7	12.3	13.3	14.6	9.4
An	83.4	87.7	77.4	87.1	86.3	84.8	90.2

texture (twinning) with augite exsolution lamellae on (001). The host low-Ca pyroxene, is partly inverted to orthopyroxene. The exsolution lamellae are thicker (up to 10 μm and widely spaced) in the core than the rims (Fig. 8). The plagioclase laths reach up to 3.2×0.3 mm in size and often include thin cores of rod- or

tube-shaped pigeonite filled with plagioclase in the center. An Na-rich tube-shaped region is present near the center of a crystal. Dusty rims are often observed.

The pyroxene compositions of Y-791186 are distributed along the same trend as in Y-792510 (Fig. 9), except for a partly heterogeneous core of Mg-rich pyroxene which shows chemical variation from $Ca_2Mg_{46}Fe_{52}$ to $Ca_2Mg_{40}Fe_{58}$. The pyroxene cores of the partly inverted pigeonite have a bulk composition of $Ca_{8.1}Mg_{37.4}Fe_{54.5}$ which is among the most Mg-rich found in the ordinary eucrites. The average composition of the rims is more Ca-rich ($Ca_{24}Mg_{35}Fe_{41}$) than that of the cores, indicating that the original crystals were zoned with subcalcic augite rims.

Y-82037,91-2 is a coarse unbrecciated eucrite with crystals ranging in size up to 1 mm across, with approximately equal modal proportions of pyroxene and plagioclase (Fig. 8). The pyroxene and plagioclase tend to be distributed unevenly, and the pyroxene often occurs as an interstitial phase. The pyroxene crystals have subrounded boundaries and show very fine exsolution lamellae of augite. They do not show clouding common in ordinary eucrites, but some dusty portions of irregular shapes remain. The plagioclase crystals are short and prismatic with rounded edges.

Part of the PTS includes a few pyroxene and plagioclase crystals that are finely fractured and show the onset of granoblastic texture (Fig. 8). The polygonal pigeonite crystals are transparent and have fine exsolution lamellae (Fig. 8). This texture appears to be correlated with the presence of rounded inclusions (up to 10 μm) and dusty regions in the plagioclase. The plagioclase crystals show weak undulose extinction.

The bulk chemical composition of the Y-82037 pyroxene is $Ca_{14}Mg_{36}Fe_{50}$ and their individual analyses range from $Ca_{6.1}Mg_{38.3}Fe_{55.6}$ to $Ca_{37.3}Mg_{30.9}Fe_{31.7}$ (Fig. 9 and Table 4). This range represents incomplete resolution of the host and lamellae due to the presence of finer exsolutions indiscernible by the EPMA electron beam

Table 6. *Chemical compositions (wt%) of ilmenite (Ilm) and chromite (Chr) in Y-791186, Y-792510 and Y-82037.*

	Y-791186	Y-792510		Y-82037			
	Ilm	Ilm	Chr	Ilm1	Ilm2	Chr1	Chr2
SiO_2	0.04	0.01	0.01	0.03	0.09	0.04	0.02
Al_2O_3	0.03	0.03	7.62	0.00	0.00	6.16	4.92
TiO_2	52.3	52.6	4.73	53.2	52.0	11.2	13.05
FeO	45.2	44.4	36.2	45.1	45.4	37.5	43.8
MnO	0.86	0.98	0.62	1.05	0.94	0.65	0.66
MgO	0.65	0.45	0.43	0.63	0.71	0.50	0.48
CaO	0.05	0.02	0.06	0.00	0.04	0.00	0.00
Na_2O	0.01	0.00	0.06	0.00	0.00	0.01	0.04
K_2O	0.01	0.01	0.02	0.00	0.00	0.00	0.00
Cr_2O_3	0.18	0.00	49.04	0.08	0.66	42.1	36.4
V_2O_3	0.00	0.00	0.70	0.00	0.17	0.62	0.82
NiO	0.06	0.00	0.07	0.06	0.05	0.02	0.04
Total	99.4	98.6	99.5	100.2	100.1	98.8	100.3

(*ca.* 3 μm). In spite of the coarse, equigranular texture of Y-82037, the exsolution lamellae are fine. The plagioclase compositional range of Y-82037 (An_{88} to An_{91}) (Table 5) is smaller than those of Y-792510, Y-791186 and Y-74356, indicating that the initial crystal growth of the plagioclase was not as rapid as those of Y-792510 and Y-791186 (Fig. 10), or that the initial zoning trend was partially homogenized.

Both Cr-spinel and ilmenite occur in Y-82037, often in close association, and in some cases ilmenite has exsolved from chromite. The concentrations of TiO_2 (11 to 17 wt%), Al_2O_3 (4 to 7%) and Cr_2O_3 (30 to 42%) in the Y-82037 chromite are variable (Table 6). The ilmenite grains contain up to 0.6 wt% Cr_2O_3 (Table 6).

4. Discussion

4.1. Mineralogy and texture of Y-74356

The mineralogy of the primary pyroxenes was briefly studied by TAKEDA (1979) and TAKEDA *et al.* (1981). The primary pyroxenes in the CC-clast and fragments in the matrix have homogeneous Mg/Fe ratios which are nearly the same as those of ordinary eucrites such as Juvinas and Millbillillie. Homogenized Mg/Fe ratios of host pigeonites (up to 1.1 mm in length) and cloudy pyroxenes indicate that the pyroxenes show a type 5 metamorphic degree (TAKEDA and GRAHAM, 1991). The MnO-FeO ratio of pyroxene in all clasts (Fig. 6) show the same trend as that of basaltic achondrites (STOLPER *et al.*, 1979). The Na-Ca variations in the matrix plagioclase are not as pronounced compared to other ordinary eucrites, indicating that plagioclase has partly equilibrated. Chromite and ilmenite compositions are also within the range of the ordinary eucrites (BUNCH and KEIL, 1971). The ilmenite lamellae in the large chromite may have formed by subsolidus annealing. We conclude that Y-74356 is a thermally annealed monomict eucrite, in spite of its unusual textural features.

Although the mineral chemistry of Y-74356 is typical of monomict eucrites, it contains a recrystallized clastic matrix similar to that of some lunar granulitic breccias. Granulitic texture forms by solid-state annealing and recrystallization. The recrystallized matrices found in some ordinary eucrites are difficult to detect on a microscopic scale (YAMAGUCHI and TAKEDA, 1994). Another characteristic feature of the matrix is the presence of light-colored feldspathic zones in the matrix, which are crushed single large plagioclase grains, indicating *in situ* brecciation. Millbillillie, a similarly recrystallized eucrite, does not have such a texture, because the clastic materials of Millbillillie are well mixed (YAMAGUCHI *et al.*, 1994). Another characteristic of Y-74356 is that this rock has more than 10% pore space. The large pore space may be the result of recrystallization of highly porous primary materials. Therefore, we classify Y-74356 as a granulitic breccia.

The GP-clasts are considered to be a secondary product for several reasons. First, the chemical compositions of pyroxene, chromite, and ilmenite are compatible with the CC-clast and mineral fragments in the clastic matrix. Secondly, the granulitic texture may form by shock (shock mosaicism; BISCHOFF and STÖFFLER, 1992) and solid-state recrystallization by heating rather than by igneous processes. Any clouding and dust within the primary pyroxene crystals may have migrated out and formed the large chromite and ilmenite grains by the heating and shock event. Augite crystals

may have formed by solid-state recrystallization or may have crystallized from a small volume of partial melt. Enhanced diffusion rates at high temperature may favor the formation of augite grains rather than lamellae in the brecciated pigeonite. The GP-areas are also found in the Juvinas eucrite (Takeda and Yamaguchi, 1991), but these are found as parts of pyroxene crystals in a lithic clast of Juvinas. Judging from the similarity to Juvinas, we suggest that the GP-clasts in Y-74356 formed from a part of the CC-clast. This interpretation is supported by the evidence that the granulitic portion is present in the part of the unbrecciated Y-82037 eucrite.

The estimated closure temperature of the GP-area ranges from 841 to 873°C (mean 857 ± 16°C) which is higher than the temperature for the primary pyroxene in the CC-clast (798°C). The range of closure temperatures is due to very fine pigeonites lamellae in some augite grains. However, the difference in the estimated pyroxene closure temperatures in the CC-clasts and the GP-clasts is significant. Probably, the higher temperature (841–873°C) is the temperature at which the separate augite grains equilibrated with host pigeonites. Therefore, the GP-area could have originated by both shock and localized reheating, or could have formed by shock during thermal metamorphism.

After this major thermal metamorphic event, this rock did not suffer any shock effects as is indicated by the lack of even minor shock features such as microfaults, small areas of brecciation, or undulatory extinction of plagioclase, although shock effects are found to be common in achondrites (Bischoff and Stöffler, 1992). This is consistent with a TEM study of Y-74356 pyroxene which revealed no evidence of strong shock effects (Takeda *et al.*, 1981).

4.2. Mineralogy and texture of Y-791186, Y-792510, and Y-82037

Y-792510 is paired with Y-791186 according to mineralogical data (Takeda, 1991) and exposure ages obtained by Nagao and Ogata (1989). Y-792510 has type-6 homogenized pyroxenes (Takeda and Graham, 1991) which cooled slowly after crystallization and probably experienced the highest thermal metamorphic grade in the ordinary eucrites. Also, a clast of Y-791186 contains type-4 pyroxene (Stannern-type; Takeda and Graham, 1991). Therefore, this rock is a mechanical mixture of two kinds of pyroxene which had different thermal histories. In contrast to Y-74356, the matrices of Y-791186 and Y-792510 are not appreciably recrystallized and, therefore, did not suffer from thermal effects. This indicates that the brecciation event occurred after the major thermal metamorphic event. The absence of thermal effects in the clastic matrix is common in polymict eucrites (*e.g.* Delaney *et al.*, 1984). The shock effects in pyroxene and feldspar crystals in Y-792510 might have been formed during brecciation or lithification. This type of ordinary eucrite was unbrecciated on a PTS scale during thermal metamorphic event. The heterogeneous distribution of the granoblastic area in the unbrecciated Y-82037 eucrite suggests that it may have experienced a shock event without brecciation on the scale of this meteorite specimen.

The recrystallized clastic matrix of Y-74356 was not found in Y-791186 or Y-792510. Y-74356 cannot be paired with other Antarctic monomict eucrites. Other ordinary eucrites, Y-82037 and Y791195 (Takeda, 1991) are unbrecciated. Since the

Table 7. Textural and mineralogical characteristics of the eucrites, Y-74356, Y-791186, Y-792510, and Y-82037.

	Y-74356	Y-791186/2510	Y-82037
Precursor rock[*1]	Monomict breccia (cataclastic?)	Unbrecciated? (>2 kinds of rocks)	Unbrecciated?
Breccia type	Granulitic breccia	Fragmental breccia	Unbrecciated
GP-area (clast)	Present	Absent (but, initial stage?)	Absent
Texture of clastic matrix	Recrystallized (Porosity >10%)	Detrital	No matrix
Pyroxene type[*2]	5	6 and 4	5
Shock feature in plagioclase	None	Undulose extinction	Undulose extinction

[*1]Breccia type during or before the major thermal event.
[*2]Takeda and Graham (1991).

matrix texture is a useful indicator in identifying pairings of meteorites, Y-74356 cannot be paired with the Y-791186 or Y-792510. The presence of a porous matrix and absence of any shock features indicates that, despite its small weight (10.0 g) recovered, Y-74356 is a unique type of ordinary eucrite; therefore, Y-74356 is a single suite and a new type eucrite among the Yamato specimens. The characteristics of these eucrites are summarized in Table 7.

4.3. Early thermal metamorphism on the parent body

Based on the above discussions, the history of Y-74356 can be summarized as follows (Table 8): (1) primary crystallization of the CC-clast pyroxene and plagioclase; (2) thermal metamorphism which yielded clouding and exsolution of pyroxene; (3) brecciation to produce the clastic matrix; and (4) prolonged thermal metamorphism to recrystallize the clastic matrix. The GP-clast might have formed at the same time during the brecciation event (3) and subsequent thermal metamorph-

Table 8. The impact and thermal history of Y-74356.

Stage		Related lithologies	Temperature (Kretz, 1982)
1	Primary crystallization	CC-clast	
2	Slow cooling	Homogenization of Mg/Fe Cloudy pyroxene	(Subsolidus)
3	Shock event	GP-clast Clastic matrix	(Subsolidus)
4	Slow cooling	Augite grain in GP-area Recrystallized clastic matrix	841–873°C ~798°C*

*Calculated from augite lamellae in CC-clast from ATEM data (Takeda et al., 1981).

ism (4). Petrographic observation of clouding and exsolved pyroxenes among eucrites is characteristics of stage 2. A significant number of non-Antarctic and Antarctic monomict eucrites have also recorded thermal metamorphism following brecciation (stage 4). Recrystallized clastic and/or melt matrix has been found in Millbillillie, Stannern, Juvinas, and Camel Donga (YAMAGUCHI and TAKEDA, 1994; METZLER et al., 1994). We now add Y-74356 to the list with recrystallized matrix.

Formation of Y-791186 and Y-792510 is explained by three stages: (1) primary crystallization; (2) slow cooling to produce homogenized pyroxene and exsolution; and (3) brecciation and small scale mixing, and lithification. The brecciation process is separate from the major thermal event in contrast to Y-74356. The rarity of impact melt breccias and granulitic breccias in ordinary eucrites is evidence for the uncommon nature of extensive brecciation prior to thermal metamorphism. These observations may also reflect a sampling bias. Only the layered texture of Millbillillie (YAMAGUCHI et al., 1994), which might have been formed by mixing of clastic materials and melts, supports the relationship between impact and thermal events. In addition, some ordinary eucrites such as Y-82037, Ibitira (STEELE and SMITH, 1976), Chervony Kut, Adalia (BASALTIC VOLCANISM STUDY PROJECT, 1981) are not brecciated. We could not find evidence that large cratering events caused major thermal metamorphism, since precursors of those specimens are not polymict breccias. However, the data presently available are ambiguous.

The textural features of the matrix of Y-74356 are similar to lunar granulitic breccias such as 79215 (e.g. TAYLOR et al., 1991). Both breccia types have a similar history of solid-state recrystallization after brecciation; they are composed of plagioclase and mafic minerals and the precursors of breccias are pristine crustal rocks. Therefore, we can deduce the early history of the Y-74356 parent body by analogy to lunar granulitic breccias. Lunar granulitic breccias can be derived by the recrystallization of the polymict breccias by heating at temperatures 1000–1150°C for $<10^3$ years (CUSHING, 1993). However, the estimated temperatures for Y-74356 (798–873°C) are lower, so the time scale of the eucrite metamorphism is much longer. On the other hand, according to MIYAMOTO et al. (1985), it takes $<10^6$ years at 1000°C to produce type-5 pigeonite (TAKEDA and GRAHAM, 1991) from extensively zoned type-2 pigeonite (TAKEDA and GRAHAM, 1991). Since most ordinary eucrites have been annealed more than type-5 (TAKEDA and GRAHAM, 1991), the thermal metamorphism was common on their parent body. In summary, the thermal metamorphism which produced the ordinary eucrites extended for longer periods of time and at lower temperature than lunar granulitic breccias.

A large cratering event is unlikely to have caused extensive thermal metamorphism on the small HED parent body, Vesta, because it may be difficult to produce sufficient impact melt on Vesta by comparison to the Moon. BISCHOFF and STÖFFLER (1992) point out that large impact melt breccias have not been reported in contrast to mesosiderites. YAMAGUCHI et al. (1994) discussed two possibilities for the heat sources: large impact cratering events and regional or parent-body-wide thermal metamorphism. We prefer the second possibility, which is highly speculative but it must be related to an early process of planetary crust formation. During the formation of the primary eucritic crust, frequent meteoroid bombardment might

brecciate the "hot" crust, and rate of extrusion of basalt flows may be very high (SCOTT *et al.*, 1989). The basalt might be metamorphosed in the hot lava. This process does not need large and intense cratering events, and it can also explain a number of "monomict eucrites" and the presence of unbrecciated eucrites (BASALTIC VOLCANISM STUDY PROJECT, 1981). A further study is required to determine the sequence of impact and thermal events recorded in many ordinary eucrites.

Acknowledgments

References

BASALTIC VOLCANISM STUDY PROJECT (1981): Basaltic volcanism on the terrestrial planets. New York, Pergamon Press, 1286p.

BENCE, A. E. and ALBEE, A. L. (1968): Empirical correction factors for the electron microanalysis of silicates and oxides. J. Geol., **76**, 382–403.

BISCHOFF, A. and STÖFLER, D. (1992): Shock metamorphism as a fundamental process in the evolution of planetary bodies: Information from meteorites. Eur. J. Mineral., **4**, 707–755.

BINZEL, R. P. and XU, S. (1993): Chips off of asteroid 4 Vesta: Evidence for the parent body of basaltic achondrite meteorites. Science, **260**, 186–191.

BUNCH, T. T. and KEIL, K. (1971): Chromite and ilmenite in non-chondritic meteorites. Am. Mineral., **56**, 146–157.

DELANEY, J. S., PRINZ, M. and TAKEDA, H. (1984): The polymict eucrites. Proc. Lunar Planet. Sci. Conf., 15th, C251-C288 (J. Geophys. Res., **89** Suppl.).

CUSHING, J. A. (1993): Thermal history of the granulitic impactite suite rocks from the lunar highlands. Master thesis. University of Hawaii at Manoa.

KRETZ, R. (1982): Transfer and exchange equilibria in a portion of the pyroxene quadrilateral as deduced from natural and experimental data. Geochim. Cosmochim. Acta, **46**, 411–421.

METZLER, K., BOBE, K.-D., PALME, H., SPETTEL, B. and STÖFFLER, D. (1994): Thermal and impact metamorphism of the HED parent body. Planet. Space Sci., **42**, (in press).

MIYAMOTO, M., DUKE, M. B. and McKAY, D. S. (1985): Chemical zoning and homogenization of Pasamonte-type pyroxene and their bearing on thermal metamorphism of a howardite parent body. Proc. Lunar Planet. Sci. Conf., 15th, C629–C635 (J. Geophys. Res., **90** Suppl.)

MORI, H. and TAKEDA, H. (1985): Oriented chromite inclusions in pigeonite crystals of eucrite meteorites. Papers Presented to the 10th Symposium on Antarctic Meteorites, March 25–27, 1985. Tokyo, Natl Inst. Polar Res., 34.

NAGAO, K. and OGATA, A. (1989): Noble gases and ^{81}Kr terrestrial ages of Antarctic eucrites. Mass Spectrosc., **37**, 313–324.

SCOTT, E. R. D., TAYLOR, G. J., NEWSOM, H. E., HERBERT, F., ZOLENSKY, M. and KERRIDGE, J. F. (1989):

Chemical, thermal and impact processing of asteroids. Asteroids II, ed. by R. P. Binzel *et al.* Tucson, Univ. Arizona Press, 701–739.

Steele, I. M. and Smith, J. V. (1976): Mineralogy of the Ibitira eucrite and comparison with other eucrites and lunar samples. Earth Planet. Sci. Lett., **33**, 67–78.

Stolper, E., McSween, H. Y., Jr. and Hay, J. F. (1979): A petrogenetic model of the relationships among achondrite meteorites. Geochim. Cosmochim. Acta, **43**, 589–602.

Takeda, H. (1979): A layered-crust model of a howardite parent body. Icarus, **40**, 455–470.

Takeda, H. (1991): Comparison of Antarctic and non-Antarctic achondrite and possible origin of the difference. Geochim. Cosmochim. Acta, **55**, 35–47.

Takeda, H. and Graham, A. L. (1991): Degree of equilibration of eucritic pyroxenes and thermal metamorphism of the earliest planetary crust. Meteoritics, **26**, 129–134.

Takeda, H. and Yamaguchi, A. (1991): Recrystallization and shock textures of old and new samples of Juvinas in relation to its thermal history. Meteoritics, **26**, 400.

Takeda, H., Miyamoto M., Duke, M. B. and Ishii, T. (1978): Crystallization of pyroxenes in lunar KREEP basalt 15386 and meteoritic basalt. Proc. Lunar Planet. Sci. Conf., 9th, 1157–1171.

Takeda, H., Mori, H., Ishii, T. and Miyamoto, M. (1981): Thermal and impact histories of pyroxene in lunar eucrite-like gabbros and eucrites. Proc. Lunar Planet. Sci., 12B, 1297–1313.

Taylor, G. J., Warren, P. H., Ryder, G., Delano, J., Pieters, C. and Lofgren, G. (1991): Lunar rocks. Lunar Source Book, A User's Guide to the Moon, ed. by G. H. Heiken *et al.* Cambridge, Cambridge Univ. Press, 183–234.

Yamaguchi, A. and Takeda, H. (1994): Granulitic matrices in monomict eucrites. Lunar and Planetary Science XV. Houston, Lunar Planet Inst., 1525–1526.

Yamaguchi, A., Takeda, H., Bogard, D. D. and Garrison, D. H. (1994): Textural variation and impact history of the Millbillillie eucrite. Meteoritics, **29**, 237–245.

Yanai, K. and Kojima, H., comp. (1987): Photographic Catalog of the Antarctic Meteorites. Tokyo, Natl Inst. Polar Res., 298p.